


Discrete R -symmetry, various energy scales, and gravitational wavesGongjun Choi¹, Weikang Lin², and Tsutomu T. Yanagida^{2,3}¹*CERN, Theoretical Physics Department, CH-1211 Genève, Switzerland*²*Tsung-Dao Lee Institute, Shanghai Jiao Tong University, Shanghai 200240, China*³*Kavli IPMU (WPI), The University of Tokyo, Kashiwa, Chiba 277-8583, Japan* (Received 20 January 2022; accepted 9 March 2022; published 30 March 2022)

We present a supersymmetric model where energy scales of a discrete R -symmetry breaking (Z_{6R}) and cosmic inflation are commonly attributed to the confinement scale of a hidden $Sp(2)$ strong dynamics. Apart from these, the supersymmetry-breaking scale, the Higgsino mass, and the right-handed neutrino masses are all shown to stem from the Z_{6R} breaking scale inferred from cosmic microwave background observables. We will show that the model is characterized by the supersymmetry-breaking soft mass $m_{\text{soft}} \simeq 100\text{--}1000$ TeV and the reheating temperature $T_{\text{rh}} \simeq 10^9$ GeV. Then we discuss how these predictions of the model can be tested with the help of the spectrum of the gravitational wave induced by the short-lived cosmic string present during the reheating era.

DOI: [10.1103/PhysRevD.105.055033](https://doi.org/10.1103/PhysRevD.105.055033)**I. INTRODUCTION**

When the Standard Model (SM) is extended by the local supersymmetry (SUSY), it is believed that SUSY is broken at an energy scale higher than the electroweak (EW) scale due to the null observation of any sparticles in the LHC. Now that the observed vanishingly small cosmological constant results from the balance between a SUSY-breaking scale and a R -symmetry breaking scale in supergravity (SUGRA), R -symmetry should have been spontaneously broken at a certain time in the history of the Universe at least prior to the EW phase transition era.

As such, R -symmetry has been subject to questions about its nature. These include whether the symmetry is local or global and continuous or discrete. A global symmetry is argued to be easily broken by quantum gravity effects so that it is difficult to be exact [1]. When applied to R -symmetry, the argument makes it difficult to discuss an R -symmetry breaking scale because the theory cannot control R -charged nonrenormalizable operators. Taking the attitude that conspiracy among fine-tuned coefficients of R -charged nonrenormalizable operators is never the decisive factor for determining an R -symmetry breaking scale, we focus our attention to a gauged R -symmetry. But it is very difficult to realize an anomaly free gauged $U(1)_R$ symmetry in the minimal SUSY SM (MSSM). Following this logic, we find that it is more probable to have the

effective theory respecting a gauged discrete R -symmetry prior to generation of a nonzero constant term in the superpotential [2,3].

On top of this, from the model building point of view, there are several merits to consider gauged discrete R -symmetries (Z_{NR} with $N \in \mathbb{Z}$ and $N > 2$). For some choices of N , the mixed anomalies of $Z_{NR} \otimes [G_{\text{SM}}]^2$ vanish within MSSM where G_{SM} is a non-Abelian gauge group in the SM [4]. For an anomaly free choice of N , the R charge of the operator $H_u H_d$ becomes 4 modulo N , which prevents the Planck scale Higgsino mass [5].¹ This fact, when combined with the requirement that R charges of Yukawa coupling operators in the SM are 2 modulo N , naturally suppresses the dangerous proton decay operator $\mathbf{10} \mathbf{10} \mathbf{10} \bar{\mathbf{5}}$ [7,8].²

The appealing idea of having a gauged discrete R -symmetry in the theory, however, finds a dangerous cosmological problem when the symmetry breaking happened after the end of inflation [9,10]: it is unavoidable that domain walls form on the spontaneous breaking of Z_{NR} . This causes the Universe to be quickly dominated by the domain wall and thus to be overclosed unless the symmetry breaking took place before the end of inflation. One may wonder whether the possibility of the breaking after the inflation can be saved with a sufficiently small explicit R -symmetry breaking term in the superpotential [11]. Once

Published by the American Physical Society under the terms of the Creative Commons Attribution 4.0 International license. Further distribution of this work must maintain attribution to the author(s) and the published article's title, journal citation, and DOI. Funded by SCOAP³.

¹We note that there can be still criticisms for taking the anomaly free conditions of discrete symmetries as one of guiding principles in low energy physics model buildings [6].

²Here for notational convenience, we borrow representation notations $\mathbf{10}$ and $\bar{\mathbf{5}}$ of $SU(5)_{\text{GUT}}$ to denote quarks and leptons in the SM.

an anomaly free Z_{NR} is gauged, however, it does not admit such a possibility. Therefore, as a resolution to the domain wall problem, requiring the symmetry breaking to take place prior to the end of inflation can provide us with a lower bound on R -symmetry breaking scale in terms of either a Hubble expansion rate during inflation or a reheating temperature. The simplest solution of the domain wall problem is to consider the situation where the R symmetry breaking dynamics drives the inflation at the same time.

On the other hand, R -symmetry is somewhat similar to spacetime symmetries in that it should be respected by every operator appearing in a superpotential. For the energy scale below the spontaneous Z_{NR} breaking, this observation may arouse an interesting question whether dimensionful parameters of operators in the superpotential can be universally explained by powers of Z_{NR} breaking scales. In light of this question, if a Z_{NR} breaking scale could be related to an inflation scale, we can dream of the fascinating scenario where energy scales of R -symmetry breaking, inflation, SUSY breaking, and several dimensionful parameters in the MSSM share the common origin.

Motivated by the aforementioned questions, in this paper, we present a model where the listed various energy scales can be explained by a Z_{6R} breaking scale (Sec. II). Our choice for Z_{6R} is based on the fact that it is the unique anomaly free discrete R -symmetry in the three-family MSSM [4]. Considering the case in which the spontaneous Z_{6R} breaking generates an inflaton potential and thus becomes connected to the inflation scale, we infer the Z_{6R} breaking scale from the inflation dynamics consistent with cosmic microwave background (CMB) observables (Sec. III). Then we further show how the infamous μ parameter (Higgsino mass) and the right-handed neutrino mass can be connected to and explained by the Z_{6R} breaking scale (Sec. IV). We shall also discuss the model's prediction on the reheating temperature and SUSY particle mass spectrum (Sec. V), which can be possibly tested by the spectrum of the gravitational wave caused short-lived cosmic strings (Sec. VI). From here on, we will use the same notation for a chiral superfield and its scalar component. The context discussed shall clarify which one is meant.

II. MODEL

In this section, we specify ingredients of our model by specifying the symmetry group and particle contents. In addition, we discuss how the spontaneous breaking of R -symmetry is realized in the model with the help of the hidden strong dynamics of $Sp(2)$. From here on, we take the Planck unit where the reduced Planck scale is set to the unity, i.e., $M_p = (8\pi G)^{-1/2} = 1$.

In addition to the SM gauge group, the symmetry group the model assumes is given by

TABLE I. Charge assignment of chiral superfields in the model under the gauge group in Eq. (2.1) and the global $U(1)_\Phi$ for the phase rotation of Φ . Φ is the inflaton chiral multiplet, H_u (H_d) the up (down)-type Higgs chiral multiplet in the MSSM and N the right-handed neutrino chiral multiplet. The parameters of the model λ_{ij} and δ_Φ are regarded as spurions.

	Φ	Q_i	S_{ij}	H_u	H_d	N	λ_{ij}	δ_Φ
$Sp(2)$	\dots	\square	\dots	\dots	\dots	\dots	\dots	\dots
Z_{6R}	+1	+1	0	x	$4-x$	0	0	0
$U(1)_\Phi$	-1	0	0	0	0	0	+2	+2
Z_4	+1	+1	+2	+2	+2	+1	0	+2

$$G = \underbrace{Sp(2) \otimes Z_{6R}}_{\text{gauge}} \otimes \underbrace{U(1)_\Phi \otimes Z_4}_{\text{global}}. \quad (2.1)$$

As will be shown, the strong dynamics of $Sp(2)$ induces the spontaneous breaking of Z_{6R} to Z_{2R} as the theory enters the confined phase.³ The particle contents and the charge assignment on them are shown in Table I. Concerning a gauged discrete R -symmetry the model obeys, we choose Z_{6R} in accordance with the merits pointed out in Sec. I. Z_4 can be regarded as a subgroup of the global $U(1)_{B-L}$ symmetry where B (L) stands for the baryon (lepton) number.

In general, for $Sp(N)$ supersymmetric gauge theory with $N_F = 2(1+N)$ being chiral superfields Q_i ($i = 1 - N_F$) transforming as the fundamental representation, the mixed anomaly of $Z_{6R} \otimes Sp(N)^2$ vanishes when the following condition is satisfied [14–16]

$$3 \times R[\lambda_a] + \frac{1}{2} \times \left\{ \sum_{i=1}^{N_F} (R[Q_i] - 1) \right\} = \frac{6}{2} \times \ell \quad (\ell \in \mathbb{Z}), \quad (2.2)$$

where $R[\lambda_a] = 1$ and $R[Q_i]$ are R charges of the gaugino and Q_i . Particularly for $N = 2$ ($N_F = 6$), we see that Eq. (2.2) holds true as long as $R[Q_i]$ is an integer. This explains our choice for $Sp(2)$ as a gauge group for the hidden strong dynamics. For an energy scale below the dynamical scale (Λ_*) of $Sp(2)$, the theory is known to be described by $(2N+1)(N+1)$ composite meson fields $\mathcal{M}_{ij} \equiv (4\pi) \langle Q_i Q_j \rangle / \Lambda_*$ with the deformed moduli constraint $\text{Pf}(\mathcal{M}_{ij}) = \Lambda_*^3$ [17].

At a high energy scale at which $Sp(2)$ is in the perturbative regime, the part of the superpotential of the theory reads

$$W_{\text{total}} \ni W_{\cancel{R}} + W_{\text{HN}}. \quad (2.3)$$

In Eq. (2.3), $W_{\cancel{R}}$ is the part of W_{total} responsible for R -symmetry breaking and the inflation

³This way of inducing the spontaneous Z_{6R} breaking is similar to the dynamical SUSY breaking based on the Izawa-Yanagida-Intriligator-Thomas mechanism [12,13].

$$W_{\not{k}} = -a_{ij}Q_iQ_jS_{ij} + \lambda_{ij}S_{ij}\Phi\Phi + \delta_\Phi\Phi\Phi, \quad (2.4)$$

where a_{ij} and λ_{ij} are dimensionless coupling constants and the sum over the repeated indices is assumed implicitly.

On the other hand, W_{HN} contains the mass terms for the Higgsino and the right-handed neutrinos⁴

$$W_{\text{HN}} = b_{ij}(Q_iQ_j)^2H_uH_d + c_{ij}Q_iQ_jNN, \quad (2.5)$$

where b_{ij} and c_{ij} are a dimensionless coupling constant. We implicitly assumed three species of the right-handed neutrinos for which there exist three different c_{ij} s.

Without loss of generality, we can choose the moduli space in the confined phase of $Sp(2)$ such that vacuum expectation values (VEVs) of Q_i fields satisfy

$$\begin{aligned} \langle Q_1Q_2 \rangle &= \langle Q_3Q_4 \rangle = \langle Q_5Q_6 \rangle = v^2 = \frac{\Lambda_*^2}{4\pi}, \\ \langle Q_iQ_j \rangle &= 0 \quad \text{for } j-i \neq 1, \end{aligned} \quad (2.6)$$

where Λ_* is the dynamical scale of $Sp(2)$. From Eq. (2.6), it becomes self-evident that the spontaneous breaking of Z_{6R} to Z_{2R} occurs when $Sp(2)$ becomes strongly coupled. In order to simplify the first term in Eq. (2.4), we make the following definition of the chiral superfield S

$$S \equiv a_{12}S_{12} + a_{34}S_{34} + a_{56}S_{56}. \quad (2.7)$$

Then in the confined phase, we can rewrite Eq. (2.4) as

$$W_{\not{k}} = -v^2S + \lambda S\Phi\Phi + \delta_\Phi\Phi\Phi, \quad (2.8)$$

where we assumed $\sum_{ij}\lambda_{ij}/a_{ij} = \lambda$ for the simplicity of the analysis.

The superpotential in Eq. (2.8) provides the scalar potential for S and Φ with account taken of the Kähler potential below,

$$K(\Phi, S) = |S|^2 + |\Phi|^2 + c_1|S|^2|\Phi|^2 + \dots, \quad (2.9)$$

where the ellipsis stands for higher powers of $|S|$ and $|\Phi|$. From here on, we assume the suppression of the higher

⁴There are more operators contributing to W_{HN} that are of the form $\sim\Phi^4H_uH_d$ and $\sim\Phi^2NN$ respecting Z_{6R} . As discussed later, when these are accompanied by the spurion fields λ_{ij} and δ_Φ , their contribution to the Higgsino and right-handed neutrino mass is comparable to operators in Eq. (2.5). Thus, for our purpose, Eq. (2.5) suffices.

order terms in $K(\Phi, S)$ above so that the three terms in Eq. (2.9) are dominant.⁵

We end this section by commenting on the values of λ and δ_Φ . As can be seen in the next section, we shall consider the case where the last term in Eq. (2.8) is irrelevant for the inflationary dynamics. Namely the last term's contribution to the inflaton potential during inflation is subdominant. However, on acquisition of a VEV of Φ at the end of inflation, the last term generates the constant term for the superpotential. Given $\langle\Phi\rangle \sim 2$ at the end of inflation, we will set δ_Φ to be of order a gravitino mass ($\sim v^4$) in order to correctly produce the vanishingly small cosmological constant. In addition, $\langle\Phi\rangle \sim 2$ at the end of inflation will further require $\lambda \sim v^2 \simeq 10^{-6}$. We take the attitude to treat δ_Φ and λ as spurions so that their smallness is originated from the breaking of the global symmetries $U(1)_\Phi$ and Z_4 shown in Table I.

III. INFLATIONARY DYNAMICS

In this section, we discuss how the dynamically generated superpotential in Eq. (2.8) and the Kähler potential in Eq. (2.9) can lead to the inflationary expansion of the early Universe [18–21] for a certain range of parameters λ and v . For the preinflationary era, we envision the situation where the Universe is dominated by the thermal bath since the Planck time $t \sim M_P^{-1}$. Starting from $T \sim M_P$, the temperature of the Universe continues to decrease in the expanding background until the inflationary era is reached. The Φ multiplet remains decoupled from the thermal bath because of the smallness assumed for $\lambda \sim v^2 \simeq 10^{-6}$, while Q , S , and the gluon multiplet of $Sp(2)$ are in thermal equilibrium, and thus $\langle S \rangle = \langle Q \rangle \sim 0$. When $T \simeq v$ is met, $Sp(2)$ theory becomes strongly coupled and Z_{6R} is broken down to Z_{2R} . Then the domain wall associated with the discrete R -symmetry breaking forms. Later when the inflaton potential energy dominates the energy at a certain spatial region, the single field slow-roll inflation gets started.

At the Planck time, in principle Φ can be any value within $[-M_P, M_P]$ because the field fluctuation is comparable to the Hubble expansion rate prior to the inflation (H_{pre}), i.e., $\delta\Phi \simeq H_{\text{pre}}/(2\pi) \sim M_P$. Now we can readily expect the presence of the spatial region containing two points x_+ and x_- separated by more than $1/H_{\text{pre}}$ with $\Phi(x_+) \simeq M_P$ and $\Phi(x_-) \simeq -M_P$. With Φ chosen monotonic within $[x_-, x_+]$, its analyticity and continuity

⁵Of course, this assumption is hardly justified in the model we present in this section since much more higher dimensional operators including higher powers of $|\Phi|$ and $|S|$ can be allowed by the symmetry of the model and thus expected to be present. Nevertheless, for our purpose of relating R -symmetry breaking scale and the inflation scale, we rely on this assumption for suppression and make the prediction of the model for the CMB observables in accordance with the assumption.

guarantee that there exists a spatial point x_0 corresponding to the zero field value ($\Phi(x_0) = 0$) inside the Hubble patch of the radius $1/H_{\text{pre}}$. Let us denote this kind of Hubble patch as H_{x_0} . As far as the Hubble patch H_{x_0} is concerned, we may regard the dynamics of Q as unaffected by Φ thanks to $|\Phi| \ll 1$ and thus naturally expect $\delta Q \lesssim H_{\text{pre}}/(2\pi)$.⁶ Given that the curvature of Φ field potential amounts to $\sim \lambda Q^2$, which is at most λH_{pre}^2 , the smallness of λ implies $\dot{\Phi} \approx 0$ especially for the spatial region near x_0 . This point assures us that the presence of x_0 within the Hubble patch H_{x_0} persists as the Universe cools down prior to the inflation.

Our inflation scenario has the advantage to avoid the initial condition problems posed either by the initial field values or large inhomogeneities [22]. One initial problem is that small field inflation models like the new inflation do not have inflationary tracker solutions, and the initial value and velocity of the inflaton need to be close to 0. We find that our inflation scenario does not suffer from this problem because of the existence of x_0 and the fact that $\dot{\Phi} \approx 0$ for the spatial region near x_0 continues by the onset of inflation. Furthermore, our inflation scenario has a large VEV of Φ as opposed to the ‘‘new inflation.’’ Therefore, to achieve a long enough inflation, the initial value of the inflaton does not have to be initially very close to 0. For the other initial condition problem, there has been the debate regarding whether the inflation can be realized even in the presence of large initial inhomogeneities. Classified as the large field inflation model with $\Delta\Phi \sim \mathcal{O}(M_P)$, our model is considered robust to the initial inhomogeneities if there is [23].

When the Universe enters the confined phase of $Sp(2)$ (still in the preinflationary era), the superpotential of Φ within the Hubble patch H_{x_0} effectively becomes of the form Eq. (2.8) and we expect the domain wall associated with Z_{6R} breaking to form around H_{x_0} .⁷ In SUGRA, the scalar potential is given by

$$V = e^K \left[\sum_{m,n} \left(\frac{\partial^2 K}{\partial X_m \partial X_n^*} \right)^{-1} D_{X_m} W D_{X_n^*} W^* - 3|W|^2 \right], \quad (3.1)$$

where X_m is a chiral superfield, the subscript on X_m distinguishes different chiral superfields and

⁶For the region where $|\Phi| \ll 1$, both Q and S have convex potentials centered on the origin of the field space. So their fluctuations are at most that of a massless scalar.

⁷For the case where the separation between the two points x_{\pm} is smaller than $1/H_{\text{pre}}$, a value of Q varies significantly within H_{x_0} . So the domain wall associated with Z_{6R} breaking may form within a Hubble patch of the radius $1/H_{\text{pre}}$. This makes the evolution of Φ in H_{x_0} unclear and complicated. It might be still probable to have the inflation in such a patch, but more rigorous exploration dealing with the coupled system of Q and Φ is needed for further discussion. Thus we focus on the opposite situation as specified in the main text.

$D_{X_m} W = (\partial W / \partial X_m) + W(\partial K / \partial X_m)$ was defined. We assume a set of coefficients of operators forming the potential of S so as to have $S = 0$.⁸ By substituting $W_{\cancel{f}}$ in Eq. (2.8) and $K(\Phi, S)$ in Eq. (2.9) into Eq. (3.1), we obtain the following potential for Φ at $S = 0$

$$V(\Phi) \simeq e^{|\Phi|^2} \left[\frac{|v^2 - \lambda\Phi\Phi|^2}{(1 + c_1\Phi\Phi)} + \delta_\Phi^2 |\Phi|^2 \right]. \quad (3.2)$$

Identifying the real part of Φ with the inflaton field, i.e., $\phi = \Phi/\sqrt{2}$ and ignoring the subdominant term, we obtain the following potential for ϕ , which is relevant for the slow rolling,

$$V(\phi) \simeq v^4 e^{\frac{\phi^2}{2}} \left(1 - \kappa \frac{\phi^2}{2} \right)^2 \left(1 + c_1 \frac{\phi^2}{2} \right)^{-1}, \quad (3.3)$$

where we defined $\kappa \equiv \lambda/v^2$.

On formation of $V(\phi)$ in Eq. (3.3), we expect that the single-field slow-roll inflation within H_{x_0} gets started with the initial inflaton field value close to zero. We have seen that the presence of x_0 in H_{x_0} can be ensured and thus the inflation can occur in H_{x_0} with $V(\phi)$ just like the topological inflation [24]. The degree of slow rolling is measured by the two parameters ϵ and η

$$\epsilon(\phi; c_1, \kappa) \equiv \frac{1}{2} \left(\frac{V'}{V} \right)^2, \quad \eta(\phi; c_1, \kappa) \equiv \left(\frac{V''}{V} \right), \quad (3.4)$$

which are functions of ϕ and depend on c_1 and κ . Let us use the subscript ‘‘ \star ’’ (‘‘end’’) for quantities evaluated at the time of the horizon exit of the CMB pivot scale (at the end of inflation). We define ϕ_{end} as a solution to the equation $\epsilon(c_1, \kappa) = 1$.

For a given set of (v, c_1, κ) and $0 < \phi_\star < 1$, using Eqs. (3.3) and (3.4), we can compute the prediction of the model for the following CMB observables including the spectral index (n_s) and the amplitude (A_s) of the power spectrum for the comoving curvature perturbation, and the tensor to scalar ratio (r) at the CMB pivot scale $k_\star = 0.05 \text{ Mpc}^{-1}$

$$A_s = \frac{1}{12\pi^2} \frac{V(\phi_\star)^3}{V'(\phi_\star)^2}, \quad n_s - 1 = -6\epsilon_\star + 2\eta_\star, \quad r = 16\epsilon_\star, \quad (3.5)$$

and the number of e -foldings during the inflation

⁸ $S = 0$ can be easily justified even by relying on the positive Hubble induced mass that drives evolution of S towards the origin of the field space.

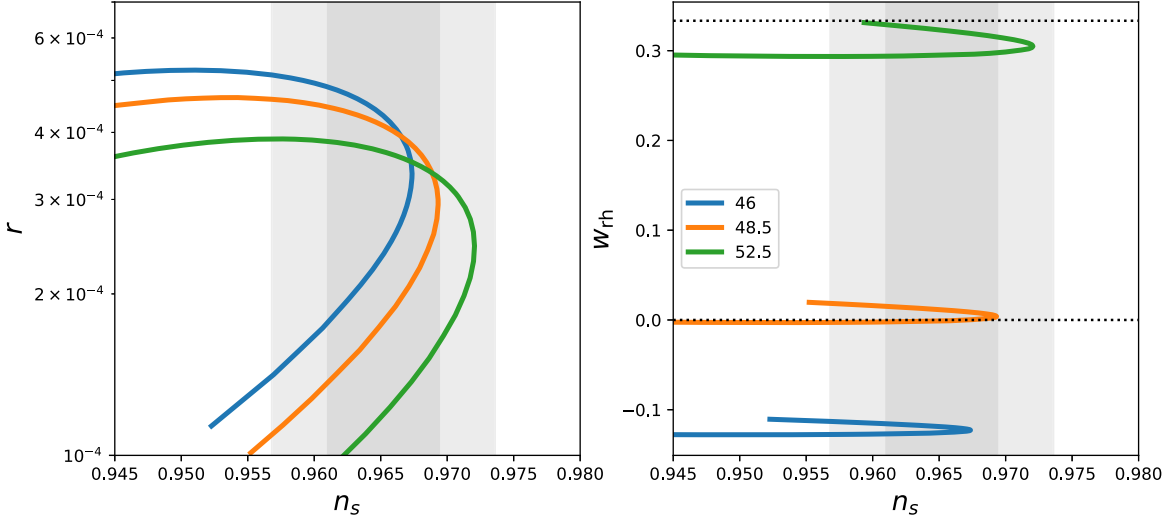


FIG. 1. Some predicted quantities in our model taking $c_1 = 0.435$. Left: the prediction of the inflation model for the scalar spectral index (n_s) and the tensor-to-scalar ratio (r) for each of the specified $N_* = 46$ (blue), 48.5 (orange), and 52.5 (green). The gray vertical bands show the 1σ and 2σ constraints of n_s . Right: the inferred reheating equation of state (w_{th}) versus n_s taking $T_{\text{rh}} \simeq 10^9$ GeV. When $0 < w_{\text{th}} < 1/3$ is considered, we can see that $48.5 \lesssim N_* \lesssim 53$.

$$N_* = \int_{t_*}^{t_{\text{end}}} H dt \simeq - \int_{\phi_*}^{\phi_{\text{end}}} \left(\frac{3H^2}{V'} \right) d\phi \simeq - \int_{\phi_*}^{\phi_{\text{end}}} \frac{V}{V'} d\phi, \quad (3.6)$$

where the slow-roll approximation $\dot{\phi} \simeq -V'/3H$ and $3H^2 \simeq V$ were used.

For these values, we adopt $A_s = 2.1 \times 10^{-9}$, $n_s = 0.9649 \pm 0.0042$ (68% C.L., Planck TT, TE, EE + lowE + lensing) [25] and $r < 0.036$ (95% C.L., BICEP/Keck) [26]. In addition, we shall see that $48.5 \lesssim N_* \lesssim 53$ for a consistent reheating scenario with $T_{\text{rh}} \sim 10^9$ GeV and a reasonable reheating equation of state.

By scanning the parameter space of (v, c_1, κ) and $0 < \phi_* < 1$, it is realized that $v \sim 1.5 \times 10^{-3}$, $c_1 \gtrsim 0.4$, $\kappa \sim 0.3$, and $\phi_* \sim 0.6$ achieve a good fit to the CMB observables. Accordingly, the inflation dynamics triggered by confined phase of $Sp(2)$ gauge theory results in the relatively low tensor-to-scalar ratio $r = \mathcal{O}(10^{-4})$. In Fig. 1, we show the prediction of the inflation model for n_s and the tensor-to-scalar ratio r corresponding to some examples of N_* .

IV. VARIOUS ENERGY SCALES

In this section, we first infer the R -symmetry breaking scale, i.e., v in Eq. (2.6), from CMB observables discussed in Sec. III. Then, by demanding that the model be able to accommodate the successful electroweak symmetry breaking (EWSB) in the SUGRA framework, we infer Higgsino mass (μ_H), gravitino mass ($m_{3/2}$), and thus SUSY-breaking scale ($M_{\text{SUSY}} = \sqrt{|F|}$). We will see that our model unifying spontaneous Z_{6R} breaking and inflationary dynamics is

actually nothing but a way of realizing the early Universe physics in the pure gravity mediation scenario [27]. As such, the model will be shown to be subject to the constraint on the reheating temperature not to have too much relic abundance of wino dark matter (DM) candidate.

In our model, the discrete R -symmetry is taken to be the origin of a variety of energy scales. As such, its breaking scale is intended to account for the only dimensionful parameter in MSSM, i.e., Higgsino mass (μ_H) along with the right-handed neutrino masses through Eq. (2.5). In accordance with this feature of the model, now we are in the position to discuss these mass scales and resultant physics in light of the value $v \sim 1.5 \times 10^{-3}$ obtained from CMB observables discussed in Sec. III.

Above all, with $H_u H_d$ having an R charge of 4, it couples to four Q chiral superfields. Thus the model predicts $\mu_H = \mathcal{O}(0.1) \times v^4 \simeq 100\text{--}1000$ TeV at the tree level.⁹ In addition, the Majorana mass terms for the right-handed neutrinos couple to two Q chiral superfields since they have zero R charge. This provides the supersymmetric right-handed neutrino mass $m_N = \mathcal{O}(0.1) \times v^2 \simeq 10^{11}\text{--}10^{12}$ GeV. Thus, the model can explain m_N required for the leptogenesis successfully with the aid of the discrete Z_{6R} symmetry.

Now given the value of Higgsino mass, it is realized that we can infer a gravitino mass $m_{3/2}$ from the two conditions for EWSB¹⁰

⁹In Eq. (2.5), we take $b_{ij}, c_{ij} = \mathcal{O}(0.1)$.

¹⁰Two conditions means the negative curvature of the Higgs potential at the origin of field space and the lower bounded potential.

TABLE II. Various energy scales which are the direct consequence of Z_{6R} symmetry. The energy scales are written in terms of the VEV of Q field, i.e., v . For the numbers of the energy scales for the dimensionful parameter, $\mathcal{O}(0.1)$ coupling constants are taken into account.

Relevant physics	Energy scale
R -symmetry breaking	v ($\sim 10^{15}$ GeV)
SUSY breaking	v^2 ($\sim 10^{12}$ GeV)
Inflation scale (H_{inf})	v^2 ($\sim 10^{12}$ GeV)
Higgsino mass (μ_H)	v^4 ($\sim 10^5$ – 10^6 GeV)
Right-handed neutrino mass (m_N)	v^2 ($\sim 10^{11}$ – 10^{12} GeV)

$$(|\mu_H|^2 + m_{H_u}^2)(|\mu_H|^2 + m_{H_d}^2) \simeq (B\mu_H)^2. \quad (4.1)$$

Because the scalar soft masses m_{H_u} , m_{H_d} , and B are of the order $m_{3/2}$ due to the SUGRA effect [28], $\mu_H = b_{ij}\langle Q_i Q_j \rangle^2 = \mathcal{O}(m_{3/2})$ should be the case. Hence, EWSB and the universal scalar soft SUSY-breaking masses of the order $m_{3/2}$ at the tree level in SUGRA give the important information for the gravitino mass of the model, i.e., $m_{3/2} \simeq \mu_H \simeq 100$ – 1000 TeV.

Once $m_{3/2}$ is known, now we can infer the SUSY-breaking scale based on the observation for the vanishingly small cosmological constant. From the leading order contribution to the potential in Eq. (3.1), the SUSY-breaking scale reads

$$M_{\text{SUSY}}^2 = |F| \simeq \sqrt{3}m_{3/2} = \mathcal{O}(0.1) \times v^4, \quad (4.2)$$

where F is the auxiliary component of a SUSY-breaking field. As a summary of our discussion thus far, we show the various energy scales resulting from the structure of the model and CMB observables in Table II.

With soft SUSY-breaking scalar masses and μ_H all comparable to $m_{3/2}$, as for the mass spectrum of the model, the one remaining question regards the gaugino masses. Then without extending the model for the SUSY-breaking mediation to the visible sector, what would be the prediction for gaugino masses in the current minimal scenario? The gaugino mass can be generated through SUGRA effect at the one-loop level (also known as the anomaly mediation) [29–31]. This means the gaugino mass is given by $|M_a| \simeq b_a(g_a^2/(16\pi^2))m_{3/2}$, where the subscript a is the group index, g_a is the gauge coupling, and b_a is the beta function coefficient at the one loop level.

With $m_{3/2} = \mathcal{O}(0.1) \times v^4$, now it is realized that this setup and mass spectrum are precisely what is envisioned in the pure gravity mediation scenario [27]. Wino becomes the lightest supersymmetric particle thereof and thus DM candidate. For the wino mass $M_2 \simeq 2.7$ TeV, the thermal relic of the wino ($\Omega_{\text{wino}}^{\text{th}}(M_2)h^2$) can explain the current DM abundance [32,33]. For a smaller M_2 leading to $\Omega_{\text{wino}}^{\text{th}}(M_2)h^2 \ll 0.12$, still the nonthermal production from

the decay of the gravitino can give rise to $\Omega_{\text{wino}}^{\text{th}}(M_2, T_{\text{rh}})h^2 \simeq 0.12$ that can explain the DM abundance today depending on T_{rh} . $\Omega_{\text{wino}}^{\text{th}}(M_2, T_{\text{rh}})h^2$ being proportional to $M_2 T_{\text{rh}}$, $\Omega_{\text{wino}}^{\text{th}}(M_2, T_{\text{rh}})h^2 \simeq 0.1$ is satisfied for $M_2 \simeq 2$ TeV and $T_{\text{rh}} \simeq 10^9$ GeV [27].

Therefore, we come to see that viability for explaining the gaugino masses within the current minimal scenario depends on whether the model can be consistent with $\Omega_{\text{DM}}h^2 \simeq 0.12$ with a proper choice of T_{rh} . From the wino mass generated via the anomaly mediation, $M_2 \simeq 300$ GeV – 3 TeV is expected. Thus, the current abundance of the wino $\Omega_{\text{wino}}h^2 = \Omega_{\text{wino}}^{\text{th}}(M_2)h^2 + \Omega_{\text{wino}}^{\text{nt}}(M_2, T_{\text{rh}})h^2$ can avoid exceeding $\Omega_{\text{DM}}h^2$ when $T_{\text{rh}} \lesssim 10^9$ GeV is satisfied.

In the naïve estimate of T_{rh} using $\Gamma_\phi \simeq H(T_{\text{rh}})$, $T_{\text{rh}} \simeq \sqrt{m_\phi} \simeq \sqrt{\kappa}v^2 = \mathcal{O}(10^{12})$ GeV up to the $\mathcal{O}(0.1)$ coupling constant factor, where m_ϕ is the effective inflaton mass read from Eq. (3.3). Thus it is not clear whether our inflation model is able to accommodate T_{rh} as small as 10^9 GeV. It is known that T_{rh} is closely related to the shape of an inflaton potential [34–36]. In the next section, we shall address this question for T_{rh} to see whether the model can explain the gaugino mass based on the anomaly mediation without any further extension in the model.

V. REHEATING

In this section, we discuss the prediction of the model for the reheating temperature T_{rh} based on the slope and the curvature of the inflaton potential in Eq. (3.3). We denote the time average value of the equation of the state of the Universe during the reheating stage by w_{rh} . We expect w_{rh} to be positive and close to 0 because the inflaton field went through the coherent oscillation after the inflation ends with the parabolic convex potential shape for $\phi > \phi_{\text{end}} > 1$ [37]. We begin with the review of the procedure to compute T_{rh} based on [35,36]. For a given w_{rh} , eventually we will see that T_{rh} is closely related to inflationary dynamics via a model's prediction discussed in Sec. III.

A. T_{rh} and w_{rh}

Let us denote the scale factor and the Hubble expansion rate at the horizon exit of comoving wave number k by a_k and H_k , respectively. Then for the pivot scale $k_\star = 0.05$ Mpc $^{-1}$, the ratio $k_\star/(a_0 H_0)$ can be written as

$$\frac{k_\star}{a_0 H_0} = \frac{a_{k_\star} H_{k_\star}}{a_0 H_0} = \frac{a_{k_\star}}{a_{\text{end}}} \frac{a_{\text{end}}}{a_{\text{rh}}} \frac{a_{\text{rh}} H_{k_\star}}{a_0 H_0}, \quad (5.1)$$

where each subscript (0, end, rh, eq) stands for the end of inflation, the end of reheating, and the matter-radiation equality. By taking the logarithm for both sides, we can rewrite Eq. (5.1) as

$$\ln\left(\frac{k_\star}{a_0 H_0}\right) = -N_\star - N_{\text{rh}} - N_{\text{R0}} - \ln\left(\frac{H_0}{H_{k_\star}}\right), \quad (5.2)$$

where we used the parametrization $(a_{\text{end}}/a_{k_\star}) = e^{N_\star}$, $(a_{\text{rh}}/a_{\text{end}}) = e^{N_{\text{rh}}}$ and $(a_0/a_{\text{rh}}) = e^{N_{\text{R0}}}$. Using the entropy conservation in the Universe from the reheating until today, one can replace $-N_{\text{R0}}$ on the right-hand side with the expression including T_{rh} . The aforesaid entropy conservation gives

$$g_{*s,\text{rh}} a_{\text{rh}}^3 T_{\text{rh}}^3 = \left(2 + \frac{7}{8} \times 2N_{\text{eff}} \times \frac{4}{11}\right) \times a_0^3 \times T_0^3, \quad (5.3)$$

where $g_{*s,\text{rh}}$ is the effective number of degrees of freedom in entropy, N_{eff} is the effective number of neutrino species and T_0 is the current photon temperature. For neutrino temperature, we used $T_{\nu 0} = (4/11)^{1/3} T_0$. By taking $N_{\text{eff}} = 3$ for simplicity, we obtain

$$N_{\text{R0}} = \ln\left(\frac{T_{\text{rh}}}{T_0}\right) - \frac{1}{3} \ln\left(\frac{43}{11g_{*s,\text{rh}}}\right). \quad (5.4)$$

From the ratio of the energy density of the Universe at reheating ρ_{rh} to that at the end of inflation ρ_{end} , we have

$$\frac{\rho_{\text{rh}}}{\rho_{\text{end}}} \simeq \frac{\frac{\pi^2}{30} g_{*s,\text{rh}} T_{\text{rh}}^4}{\frac{3}{2} V_{\text{end}}} = e^{-3N_{\text{rh}}(1+w_{\text{rh}})}, \quad (5.5)$$

where we used $\rho \propto a^{-3(1+w_{\text{rh}})}$ during the reheating era. Also for the relation between ρ_{end} and V_{end} , we used the fact that the kinetic energy is approximately half of the potential energy at the end of inflation defined by $\epsilon = 1$.¹¹ Equation (5.5) allows one to express T_{rh} in terms of N_{rh} and V_{end} , i.e.,

$$T_{\text{rh}} = 1.46 \times \left(\frac{V_{\text{end}}}{g_{*s,\text{rh}}}\right)^{1/4} e^{-3N_{\text{rh}}(1+w_{\text{rh}})/4}. \quad (5.6)$$

Finally the substitution of Eqs. (5.6) and (5.4) into Eq. (5.2) yields the number of the e -foldings during the reheating era

¹¹For ρ_{end} , we can in principle solve the equation of motion for ϕ with different initial conditions to obtain the relation between ρ_{end} and V_{end} . While their exact numerical relation is not needed here, we follow [36] and approximately identify the end of inflation with $w = (K - V)/(K + V) \simeq -1/3$. It then follows $K = (1/2)V$ and thus $\rho_{\text{end}} \simeq (3/2)V_{\text{end}}$.

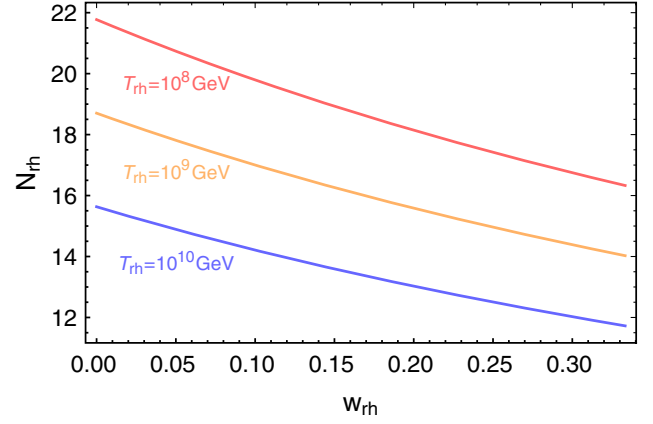


FIG. 2. The relation between the equation of state of the Universe during the reheating era (w_{rh}) and the number of the e -foldings during reheating era for $g_{*s,\text{rh}} = 230$ and $V_{\text{end}} \simeq 3 \times 10^{-12}$.

$$\begin{aligned} N_{\text{rh}} &= \frac{4}{1 - 3w_{\text{rh}}} \\ &\times \left[-N_\star - \ln\left(\frac{k_\star}{a_0 T_0}\right) + \ln\left(\frac{g_{*s,\text{rh}}^{1/4}}{g_{*s,\text{rh}}^{1/3}}\right) - \frac{1}{4} \ln(V_{\text{end}}) \right. \\ &\quad \left. + \frac{1}{2} \ln\left(\frac{\pi^2 r A_s}{2}\right) + 7.5 \times 10^{-2} \right] \\ &\equiv \frac{4}{1 - 3w_{\text{rh}}} \times [-N_\star + N_{\text{upper}}], \end{aligned} \quad (5.7)$$

where N_{upper} is all but $-N_\star$ in the square bracket in Eq. (5.7). As promised, for a given w_{rh} , we see that the prediction of an inflation model for N_\star , r , A_s , and V_{end} can determine N_{rh} in Eq. (5.7) and thus T_{rh} in Eq. (5.6).

B. Is $T_{\text{rh}} \lesssim 10^9$ GeV consistent with the model?

As was pointed out in the last part of Sec. IV, as long as $T_{\text{rh}} \lesssim 10^9$ GeV can be realized, the model can maintain the current minimal form without asking more fields either to generate gaugino mass through other mediation mechanisms than the anomaly mediation or to have an alternative DM candidate. If not (T_{rh} cannot be smaller than 10^9 GeV), the model should be extended so as to have a new lightest supersymmetric particle and DM candidate other than the wino. In this section, we address this issue by computing the model's prediction for T_{rh} based on Sec. VA.

For checking the consistency, we first attend to the relation between N_{rh} and w_{rh} in Eq. (5.7). For the inflaton potential explaining the CMB observables, we find that $V_{\text{end}} \simeq 3 \times 10^{-12}$. Then substituting this V_{end} and $g_{*s,\text{rh}} \simeq 230$ in MSSM into Eq. (5.7), we obtain the relation between N_{rh} and w_{rh} for each T_{rh} . This is shown in Fig. 2. One can see that the smaller T_{rh} requires the larger N_{rh} for a fixed w_{rh} .

On the other hand, N_{upper} in Eq. (5.7) is approximately 53 for $A_s = 2.1 \times 10^{-9}$, $r = \mathcal{O}(10^{-4})$, and $V_{\text{end}} \simeq 3 \times 10^{-12}$. Because of the rapid coherent oscillation of the inflaton field with an approximately quadratic potential after the inflation ends, we expect that w_{rh} is close to 0 for most of the time till the end of reheating. But considering details of the end of inflation and the process of reheating, we conservatively take $0 \lesssim w_{\text{rh}} \lesssim 1/3$ and so N_* smaller than ~ 53 is required for making N_{rh} positive in Eq. (5.7).

Therefore, the inflation model in Sec. III with $v \sim 1.5 \times 10^{-3}$ can be consistent with T_{rh} as small as 10^9 GeV insofar as a set of (N_*, w_{rh}) produces a large enough N_{rh} , i.e., at least $N_{\text{rh}} \gtrsim 14$. Observing Eq. (5.7) closely, one may think that having T_{rh} as small as what one desires in the model (or $N_{\text{rh}} \gtrsim 14$) is not difficult by requiring w_{rh} to be close to $1/3$. However, given that w_{rh} parametrizes the time-averaged value of the actual time-evolving equation of state of the Universe during the reheating state, we expect w_{rh} to deviate from (smaller than) $1/3$. Also, we found that satisfying CMB observations alone (especially the constraint on n_s) already requires $N_* \gtrsim 42$.

For these reasons, it is nontrivial to see whether N_{rh} , allowing for T_{rh} to be as small as 10^9 GeV, can be obtained while being consistent with all CMB observations. Given this question for the consistency, we go through the procedure to compute T_{rh} based on Sec. VA. And we confirmed that our inflation model characterized by $v = 1.5 \times 10^{-3}$ and $r = \mathcal{O}(10^{-4})$ can indeed give rise to T_{rh} as small as 10^9 GeV for $0 \lesssim w_{\text{rh}} < 1/3$ with $48.5 \lesssim N_* \lesssim 53$, which is shown in the right panel of Fig. 1.¹² Especially for w_{rh} close to 0, we found that $N_* = 48.5\text{--}49$ is needed.

The larger w_{rh} makes it easier for the model to have the smaller T_{rh} . Now that $T_{\text{rh}} \lesssim 10^9$ GeV can be indeed realized, the gaugino mass in the model can be explained based on the anomaly mediation and the wino can be the DM candidate. In the next section, we study another way of probing T_{rh} based on the spectrum of gravitational wave (GW) sourced by the short-lived cosmic string present during the reheating era.

We end this section by pointing out a potential main channel for the inflaton decay for the case of $T_{\text{rh}} \simeq 10^9$ GeV. In the Kähler potential, we may expect the nonrenormalizable operator $\mathcal{O}_{\Phi N} = c_{\Phi N} |\Phi|^2 |N|^2$ with $c_{\Phi N} = \mathcal{O}(1)$. Now that the decay rate of the inflaton due to the operator $\mathcal{O}_{\Phi N}$ reads $\Gamma(\phi \rightarrow 2N) \simeq (m_N/M_P)^2 (m_\phi/8\pi) \simeq 1$ GeV, the comparison $\Gamma(\phi \rightarrow 2N) \simeq H$ yields $T_{\text{rh}} \simeq 10^9$ GeV. Therefore, $T_{\text{rh}} \simeq 10^9$ GeV can be understood in the perturbative reheating case thanks to the large enough $m_N = 2c_{ij} \langle Q_i Q_j \rangle$ (and thus $R[N] = 0$). We notice that the consistency of the model with $(T_{\text{rh}}, m_N) \simeq (10^9 \text{ GeV}, 10^{11-12} \text{ GeV})$ is remarkable in the context of

¹²Also the model is further specified by $g_{*,\text{rh}} = g_{*,s,\text{rh}} \simeq 230$, $c_1 \gtrsim 0.4$, $\kappa \sim 0.3$, $\phi_* \sim 0.6$, and $\phi_{\text{end}} \sim 2$.

the seesaw mechanism for neutrino masses [38–41] and the primordial leptogenesis [42,43].

VI. GRAVITATIONAL WAVE: A POTENTIAL SMOKING-GUN FEATURE IN THE FUTURE

The scalar potential of a SUSY model is contributed by F terms and D terms. For a renormalizable scalar potential, there can be a direction in the space of complex scalars along which the potential vanishes as far as SUSY is respected. This direction is referred to as a “flat direction” and the collection of such directions form the so-called moduli space. The flat directions, however, are lifted when soft masses for scalars are generated on SUSY breaking.

Particularly for MSSM, before the SUSY breaking takes place, there are many almost flat directions which can be conveniently characterized by gauge invariant monomials [44]. The correspondence between flat directions and gauge invariant monomials underlies this fact [45–47] and thereby the study of dynamics of a flat direction reduces to understanding gauge invariant operators and the scalar potential stemming from those. After the SUSY breaking, flat directions are lifted since there appear unavoidable soft mass terms $m_{\text{soft}}^2 |\sigma|^2$ in the scalar potential where σ collectively denotes the scalar components of chiral superfields.

Given that flat directions are so common in the SUSY theories, one may wonder if their dynamics can be used to test predictions of a SUSY model. Concerning this, the Hubble induced mass that the flat directions receive during the inflation and the reheating times could play a critical role. Suppose the sign of the coupling $|S|^2 |\Sigma|^2$ is positive while that of the coupling $|\Phi|^2 |\Sigma|^2$ is negative where Σ is a flat direction and S and Φ fields are defined in Eq. (2.8). This gives rise to the situation where the sign of the Hubble induced mass is positive during the inflation while it is negative during the reheating stage.¹³ Then a flat direction obtains a nonzero VEV after the inflation ends although it stays at the origin of the field space during the inflation. This implies that there can be formation of cosmic strings (CS) provided chiral superfields making up a gauge invariant monomial of interest carry a global $U(1)$ charge. If so, the GW generated by the CS can contain information for m_{soft} . This is because the CSs are expected to disappear once the Hubble expansion rate during the reheating era becomes comparable to m_{soft} . Namely, the time when the generation of GWs ceases is determined by m_{soft} , which might be imprinted in the spectrum of the GW.

In [51,52], precisely this possibility was considered and it was confirmed via the simulation that the CS network

¹³The opposite situation is assumed in the Affleck-Dine baryogenesis scenario [48] and in the case where the primordial coherently oscillating scalar initiates the dark sector particles (see, for instance, [49,50]).

forms and reaches the scaling regime prior to disappearance of the CSs. On top of that, it was also studied how T_{rh} and m_{soft} can be read from the spectrum of GW spectra generated by CSs. Now having the model featured by $m_{\text{soft}} \simeq 100\text{--}1000$ TeV and $T_{\text{rh}} \lesssim 10^9$ GeV, in this section, we study how the prediction of the model can be imprinted in the GW possibly generated by the short-lived CSs originated from the temporary breaking of a global $U(1)$ symmetry. We will see that Einstein Telescope (ET) and Cosmic Explorers (CE) can be used to probe our scenario via GW detection.

A. Flat direction and cosmic string formation

In this section, first, we point out the richness of flat directions which can obtain time independent VEVs determined by the Kähler potential rather than the superpotential. After that, we compute the VEV of flat directions of our interest. The VEV lasts during the reheating era until the time when $H \simeq m_{\text{soft}}$ is reached. We consider the situation wherein the spontaneous breaking of the global $U(1)_B$ (baryon charge) is induced by the VEV and also results in the formation of the global CSs. On disappearance of the VEV, CSs do as well and thus CSs are of the short-lived kind.

In our model, as was specified in Table I, R charges of H_u , H_d , and N are given by $R[H_u] + R[H_d] = 4$ and $R[N] = 0$. Along with these, the requirement that three Yukawa coupling operators have total R charge of 2 mod 6 can fully determine R charges of the MSSM matter sector consisting of $\mathbf{10}$, $\bar{\mathbf{5}}$, H_u , H_d , and N : $R[\mathbf{10}] = 0$, $R[\bar{\mathbf{5}}] = 0$, $R[H_u] = 2$, $R[H_d] = 2$, $R[N] = 0$.¹⁴

Given the concrete R -charge assignment, we encounter one remarkable consequence of the model concerning the contribution of a flat direction to the superpotential. That is, whenever the flat directions associated with gauge invariant monomials made of $\mathbf{10}$ and $\bar{\mathbf{5}}$ appear in the superpotential, both renormalizable and nonrenormalizable operators of the flat directions must be accompanied by the suppression by the factor $(m_{3/2}/M_P) \sim 10^{-12}$. This is because the R charge of an operator in the superpotential should be 2 mod 6.¹⁵

Let us refer to the flat direction associated with gauge invariant monomials made of $\mathbf{10}$ and $\bar{\mathbf{5}}$ as χ . In Table 3 of [44], one can find gauge invariant monomials in MSSM that can be used to write any gauge invariant polynomial in $(q, \ell, \bar{u}, \bar{d}, \bar{e}, H_u, H_d)$. As an exemplary operator, we may

¹⁴For convenience, we use representations of $SU(5)_{\text{GUT}}$ to refer to these field, i.e., $\mathbf{10} = (q, \bar{u}, \bar{e})$, $\bar{\mathbf{5}} = (\bar{d}, \ell)$. Each field denotes quark $SU(2)_L$ doublet (q), lepton $SU(2)_L$ doublet (ℓ), up-quark $SU(2)_L$ singlet (\bar{u}), down-quark $SU(2)_L$ singlet (\bar{d}), lepton $SU(2)_L$ singlet \bar{e} , and up and down type Higgs (H_u and H_d).

¹⁵Some operators in the superpotential are suppressed by Z_4 symmetry given in Table I since Z_4 charges are 1 for $\mathbf{10}$ and $\bar{\mathbf{5}}$.

attend to $\bar{u}\bar{d}\bar{d}$. χ being as the flat direction of $\bar{u}\bar{d}\bar{d}$, its superpotential is given by

$$W_\chi = \left(\frac{m_{3/2}}{M_P}\right) \sum_{p=3} a_{\chi,p} \frac{\chi^p}{M_P^{p-3}} \\ \rightarrow V(\chi) \ni \left(\frac{m_{3/2}}{M_P}\right)^2 \sum_{p=3} a_{\chi,p}^2 \frac{\chi^{2p-2}}{M_P^{2p-6}} \quad (p \in \mathbb{Z}), \quad (6.1)$$

where $R[m_{3/2}] = 2$ and $R[\chi^p] = 0$, and $a_{\chi,p}$ is a dimensionless coefficient. Here we wrote M_P explicitly for the clarity. When compared to a term of the same mass dimension from Kähler potential, due to $m_{3/2} \ll H$ before CSs disappear [see Eq. (6.3)], contributions to $V(\chi)$ in Eq. (6.1) are negligible for determining the VEV of χ . Hence, it is Kähler potential that determines the VEV of χ in our model.

This result applies not only to the flat direction of $\bar{u}\bar{u}\bar{d}$ but to any flat direction associated with gauge invariant monomials purely composed of $\mathbf{10}$ and $\bar{\mathbf{5}}$. And this ensures the richness of flat directions which can potentially satisfy conditions for the signs of the Hubble induced masses we require. This unavoidable feature works in model's favor in terms of the strength of GW signal induced by the short-lived CSs. In [52], the resultant GW spectra were studied for each of the cases differentiated by which one determines the VEV of a flat direction among superpotential or Kähler potential. It turns out that the information for m_{soft} and T_{rh} can be imprinted in GW spectra equally for both cases. However, the strength of the GW spectra is relatively larger when Kähler potential determines the VEV of a flat direction. This fact renders our model more advantageous in justifying the higher chance of producing the larger GW signal in comparison with other SUSY models. Again this is essentially attributable to the assumed discrete gauged Z_{6R} symmetry.

With the assumed positive Hubble induced mass and also m_{soft} generated at the end of the inflation, χ is expected to sit in the origin of the field space during inflation. After inflation ends, the reheating era gets started and we consider the following Kähler potential of χ

$$K \supset \frac{a_2}{M_P^2} |\Phi|^2 |\chi|^2 + \frac{a_n}{M_P^{2n-2}} |\Phi|^2 |\chi|^{2n-2}, \quad (6.2)$$

where a_2 (a_n) are dimensionless coefficients of operators of mass dimension 4 ($2n$), and n is a positive integer greater than 2. After integrating over the superspace coordinates, there arise terms including $|\dot{\phi}|^2$, which result in the following potential for χ

$$V(\chi) = \left[\frac{3a_2}{2} H^2 + m_{\text{soft}}^2 \right] |\chi|^2 + \frac{3a_n}{2} H^2 \frac{|\chi|^{2n-2}}{M_P^{2n-4}}, \quad (6.3)$$

where we used the equipartition of the energy density of ϕ during oscillation, i.e., $|\dot{\phi}|^2/2 = \rho_\phi/2 \simeq (3/2)H^2 M_P^2$.

Given $H_{\text{inf}} \simeq v^2 \simeq 10^{12}$ GeV and $m_{\text{soft}} \simeq 100\text{--}1000$ TeV, it can be seen easily that the Hubble induced mass dominates over the soft mass term from the end of inflation to the time when $H \simeq m_{\text{soft}}$ is reached. If $a_2 < 0$ and $a_n > 0$ hold, then the flat direction obtains the non-vanishing VEV:

$$\langle |\chi| \rangle = \left(\frac{|a_2|}{a_n(n-1)} \right)^{\frac{1}{2n-4}} M_P. \quad (6.4)$$

Note that this VEV is independent of time. Once this VEV is acquired by the flat direction, which is a linear combination of squarks or sleptons, $U(1)_B$ symmetry becomes spontaneously broken and this temporary breaking lasts until the time when the two terms in the square bracket in Eq. (6.3) are comparable is reached. At this time ($t = t_{\text{decay}}$), the cosmic string starts to decay as $V(\chi)$ becomes the positive curvature potential. Accordingly, χ starts to oscillate around $\chi = 0$ and eventually sits at the origin.¹⁶

B. GW spectrum and testing the model

The current spectrum of the GW ($\Omega_{\text{GW}} h^2(f, t_0)$) induced by the CS that exists since the end of the inflation ($t = t_{\text{end}}$) until the time of $H \simeq m_{\text{soft}}$ ($t = t_{\text{decay}}$) is characterized by three ranges of Fourier modes: modes entering the horizon at (i) $t < t_{\text{decay}}$, (ii) $t_{\text{decay}} < t < t_{\text{rh}}$, and (iii) $t > t_{\text{rh}}$, where t_{rh} is the time when the temperature of the Universe reaches T_{rh} . These three regimes are distinguished by f_{peak} and f_{rh} . The former (later) is the GW frequency today corresponding to the k mode that reentered the horizon at the time when CSs decay (when $T \simeq T_{\text{rh}}$ holds).¹⁷

For the first regime of k reentering the horizon at the time when the CSs form, reach the scaling regime, and decay ($k \gtrsim k_{\text{peak}}$), the time evolution of the GW energy density was studied in [52] by solving the time evolution equation of χ numerically.¹⁸ With Ω_{GW} defined in Eq. (A3), $d\Omega_{\text{GW}}/d \log \tau$ was found to have a peak (GW energy production is most efficient) at k of which size is equal to $\sim 40\%$ of the comoving Hubble radius. Because of that, $\Omega_{\text{GW}}(\tau)$ has a peak that keeps shifting to the smaller k

(larger length scale) with time until t_{decay} is reached. Since then, the comoving k mode at the peak (k_{peak}) is frozen and the redshifted peak structure remains to date.

The GW energy density at k_{peak} today reads [52]

$$\Omega_{\text{GW}}^{\text{peak}} h^2 \simeq 5 \times 10^{-9} \left(\frac{|a_2|^{-1/2} m_{\text{soft}}}{10^3 \text{ TeV}} \right)^{-2/3} \times \left(\frac{T_{\text{rh}}}{10^9 \text{ GeV}} \right)^{4/3} \left(\frac{|a_2|}{a_n(n-1)} \right)^{\frac{2}{n-2}}, \quad (6.5)$$

and the corresponding peak frequency today is

$$f_{\text{peak}} \simeq 7000 \text{ Hz} \left(\frac{|a_2|^{-1/2} m_{\text{soft}}}{10^3 \text{ TeV}} \right)^{1/3} \left(\frac{T_{\text{rh}}}{10^9 \text{ GeV}} \right)^{1/3}. \quad (6.6)$$

Next, for the other regime of k reentering the horizon at the time $t > t_{\text{decay}}$, the GW spectrum can be obtained from Eq. (A15) with the numerically computed Eqs. (A7) and (A8). Before reheating completes, the equation of state of the Universe is w_{rh} while it is $1/3$ after the reheating completes. This means that, particularly for w_{rh} as small as 0, the k dependence of Ω_{GW} for $k < k_{\text{rh}}$ and $k \gtrsim k_{\text{rh}}$ is expected to be clearly distinguishable [56,57] due to different dilution of Ω_{GW} . In [52], the $w_{\text{rh}} \simeq 0$ case was studied.

For our model, as we discussed in Sec. VA, in principle any value lying in $0 \lesssim w_{\text{rh}} < 1/3$ can be possible, but w_{rh} being close to 0 is more realistic. For the purpose of the potential clear bending signature of Ω_{GW} , from here on we focus on the case with $w_{\text{rh}} \simeq 0$ but with $T_{\text{RH}} = 10^8\text{--}10^9$ GeV.

Based on $f_{\text{GW}} = k/(2\pi a_0)$ and the entropy conservation, the GW frequency today corresponding to k_{rh} reads

$$f_{\text{rh}} = \left(\frac{g_s(t_0)}{g_s(t_{\text{rh}})} \right)^{1/3} \left(\frac{T_0}{T_{\text{rh}}} \right) \frac{k_{\text{rh}}}{2\pi a_{\text{rh}}} \simeq 30 \text{ Hz} \left(\frac{T_{\text{rh}}}{10^9 \text{ GeV}} \right), \quad (6.7)$$

where we used $k_{\text{rh}} = a_{\text{rh}} H(a_{\text{rh}})$ for the second equality. At the frequency in Eq. (6.7), $\Omega_{\text{GW}}(k)$ is expected to reveal the bending due to different k dependence ascribable to the change in the equation of state of the Universe before and after the reheating.

In Fig. 3, we show the GW spectra corresponding to various different cases of $(T_{\text{rh}}, m_{\text{soft}})$. For $f < f_{\text{peak}}$, we numerically compute $\Omega_{\text{GW}} h^2$ in accordance with the Appendix with the constant T_{ij}^{TT} .¹⁹ For $f > f_{\text{peak}}$, we can obtain $\Omega_{\text{GW}} h^2$ based on the fact that $\Omega_{\text{GW}} \propto f^{-2}$ [52] and the use of Eqs. (6.5) and (6.6). For both panels, $a_2 = a_n = 1$ and $n = 3$ are commonly assumed. Solid lines show the GW spectra, whereas the dashed lines are the

¹⁶In our work, we focus on flat directions including third generation quark fields like $\bar{u}_3 \bar{d}_2 \bar{d}_3$ where the subscripts are generation indices. This makes the one-loop correction to the scalar potential dominated by that due to Yukawa interaction. In this case, the scalar potential is steeper than the quadratic one [53], preventing the B-ball formation after CSs disappear.

¹⁷Note that for T_{rh} and m_{soft} of our interest, $T_{\text{max}} \simeq 0.5 \times T_{\text{rh}}^{-1/2} H_{\text{inf}}^{1/4} M_P^{1/4}$ [54,55] is larger than the temperature when $H \simeq m_{\text{soft}}$ holds. Thus, there can be indeed the time interval when CSs form and exist prior to their decay.

¹⁸In [52], the oscillation domination was assumed, i.e., $H \propto a^{-3/2}$ and $w_{\text{rh}} = 0$, in performing the lattice simulation for solving the time evolution equation of χ . Nevertheless, the presence of the scaling regime is expected not to be affected even for w_{rh} other than 0 as long as $w_{\text{rh}} > -1/3$. We are grateful to M. Yamada for pointing out this.

¹⁹The modes satisfying $k < k_{\text{peak}}$ were outside of the horizon when GW was generated by CSs. For those superhorizon modes, the lack of causality makes T_{ij}^{TT} independent of k .

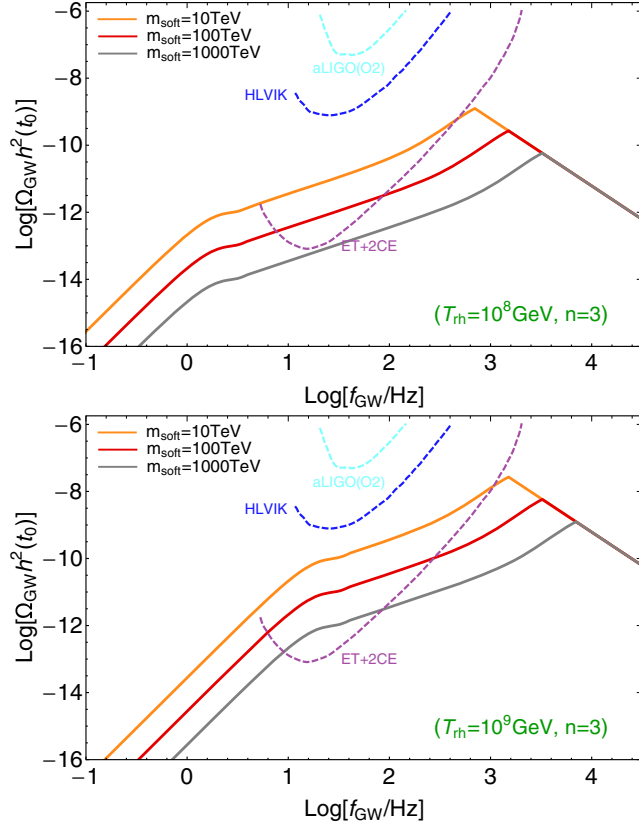


FIG. 3. GW spectra for different T_{rh} and m_{soft} . For both panels, $a_2 = a_n = 1$ and $n = 3$ are commonly assumed. Also each of the solid lines with yellow, red, and gray colors corresponds to $m_{\text{soft}} = 10, 100,$ and 1000 TeV. The upper (lower) panel shows the case with $T_{\text{rh}} = 10^8$ GeV (10^9 GeV).

sensitivity curves of upcoming GW experiments. Solid lines of different colors correspond to the specified $m_{\text{soft}} = 10$ (yellow), 100 (red), and 1000 TeV (gray). The sensitivity curve (purple dashed) of the ET [58] and two third-generation CE [59] is read from [60]. We also show the sensitivity curves of the Advanced LIGO O2 (cyan dashed) [61] and HLVIK (blue dashed) [62–65].²⁰ The upper (lower) panel shows the case with $T_{\text{rh}} = 10^8$ GeV (10^9 GeV).

We see that ET + 2CE may have a chance to see the GW spectrum induced by the short-lived cosmic strings provided T_{rh} is as large as 10^8 – 10^9 GeV and $m_{\text{soft}} = 10$ – 1000 TeV. Particularly, for $T_{\text{rh}} \simeq 10^9$ GeV, the bending at f_{rh} can be seen by ET + 2CE, which can tell us the value of T_{rh} directly via Eq. (6.7). Ideally, for the case where both $\Omega_{\text{GW}}^{\text{peak}} h^2$ and $\Omega_{\text{GW}}^{\text{bend}} h^2$ are within the sensitivity curve at $f = f_{\text{peak}}$ and $f = f_{\text{rh}}$, respectively,

²⁰HLVIK is the network of several terrestrial GW detectors including Advanced LIGO Hanford, and Livingston, Advanced Virgo, LIGO India, and KAGRA.

m_{soft} and T_{rh} can be directly read from Eqs. (6.5)–(6.7). However, we can see that the bending at f_{rh} is easier to observe, e.g., for $T_{\text{rh}} = 10^9$ GeV. We find to a good approximation that $\frac{\Omega_{\text{GW}}^{\text{bend}}}{\Omega_{\text{GW}}^{\text{peak}}} \simeq 0.365 \frac{f_{\text{rh}}}{f_{\text{peak}}}$, and so

$$\Omega_{\text{GW}}^{\text{bend}} h^2 \simeq 7.8 \times 10^{-12} \left(\frac{|a_2|^{-1/2} m_{\text{soft}}}{10^3 \text{ TeV}} \right)^{-1} \left(\frac{T_{\text{rh}}}{10^9 \text{ GeV}} \right)^2 \times \left(\frac{|a_2|}{a_n(n-1)} \right)^{\frac{2}{n-2}}. \quad (6.8)$$

Thus, even if we can only resolve the bending in the GW spectrum, we will be able to infer both T_{rh} and m_{soft} with Eqs. (6.7) and (6.8).

It is worth pointing out that the feature that the peak and bending locations correlate with their amplitudes in such a way that is difficult to be realized in other models. While such a GW spectrum is not a necessary prediction, it would be a smoking gun for our model once the two characteristic frequencies are observed in the future.

VII. CONCLUSIONS

Discrete R -symmetry Z_{NR} ($N \in \mathbb{Z}$) is a very interesting possibility in SUSY models in that its anomaly free conditions can be satisfied within MSSM. Particularly Z_{6R} is special in that it is the unique Z_{NR} that is free of the mixed anomalies for three generations of quarks and leptons in MSSM. Should the discrete R -symmetry play an important role in low energy physics, however, the relevant domain wall problem becomes a severe issue since discrete symmetries are most probably gauged [66].

On the other hand, R -symmetry is analogous to space-time symmetries in that every operator in the superpotential has to respect the R -symmetry. This fact may indicate an interesting possibility that some of dimensionful parameters in SUSY models can be powers of a R -symmetry breaking scale. Put it another way, knowing that R -symmetry must be broken in SUGRA for having a constant term in the superpotential and the breaking should be induced by a field with a nonzero R charge, we may imagine the situation in which some dimensionful parameters are nothing but spurions of the broken R -symmetry in low energy physics.

Motivated by these points, in this work, we considered the possibility in which the gauged Z_{6R} is spontaneously broken by the formation of the condensation $\langle QQ \rangle$ in the confinement of the hidden strong dynamics of $Sp(2)$ prior to the inflationary era. The breaking at the energy scale $\sqrt{\langle QQ \rangle} \simeq v \simeq 1.5 \times 10^3$ in turn drives the new inflation type potential with the VEV of the inflaton $\langle \Phi \rangle \simeq 2$. With the nonzero $R[Q] = +1$, powers of the $Sp(2)$ invariant QQ couple to $H_u H_d$ and NN so that the confinement of the hidden strong dynamics of $Sp(2)$ also generates Higgsino

mass $\mu_H \sim \langle QQ \rangle^2 \sim v^4$ and the right-handed neutrino masses $m_N \sim \langle QQ \rangle \sim v^2$. Embedded in SUGRA framework, the model predicts the scalar soft masses of order $m_{3/2}$ and EWSB further requires $\mu_H = \mathcal{O}(m_{3/2})$. Therefore, the model accounts for five energy scales for the inflation, the R -symmetry breaking, the SUSY breaking, the Higgsino mass and the right-handed neutrino mass based on the common single origin, i.e., spontaneous R -symmetry breaking before inflationary era. This result is summarized in Table I.

The model being along the same line as the pure gravity mediation scenario [27], it has wino as the DM candidate in its minimal form. For avoiding the overclosure of the Universe due to too much abundance of wino DM, $T_{\text{rh}} \lesssim 10^9$ GeV is required. We confirmed that the model can indeed lead to T_{rh} as small as 10^9 GeV as far as w_{rh} can be close to zero (see Sec. V).

Finally, in Sec. VI, we discussed the GW spectra induced by the short-lived CSs, which can be a potential smoking gun experimental signal of the model. As is the case for other SUSY models, there can be many flat directions in the model characterized by gauge invariant monomials. If the flat direction associated with a gauge invariant monomial made of squark and slepton fields couples to S and Φ with a positive and a negative coupling constant, respectively, in the Kähler potential, then there can be temporary CSs that are present since the end of inflation until the time when $T \simeq T_{\text{rh}}$ is satisfied. If this is the case, the information for m_{soft} and T_{rh} can be imprinted in the GW spectra caused by the shorted-lived CSs [51,52]. The noticeable consequence of the model is that the VEV of the flat direction is determined by the Kähler potential. This guarantees the strength of the GW spectra large enough to be detected by upcoming GW experiments including the ET and CE (see Fig. 3).

ACKNOWLEDGMENTS

G. C. is grateful to M. Yamada for the discussion about GW induced by the short-lived CSs. T. T. Y. is supported in part by the China Grant for Talent Scientific Start-Up Project and by Natural Science Foundation of China under Grant No. 12175134 as well as by World Premier International Research Center Initiative (WPI Initiative), MEXT, Japan.

APPENDIX: COMPUTATION FOR THE GW SPECTRUM

In this section, we make a review of the way to compute the spectrum of the GW sourced by the short-lived cosmic string based on [52,67,68]. For more details, we refer the readers to [52].

In the Friedmann-Robertson-Walker background, the GW is the traceless ($h^i_i = 0$) and transverse ($\partial^i h_{ij} = 0$) tensor fluctuation h_{ij} , as can be seen in

$$ds^2 = a(\tau)^2[-d\tau^2 + (\delta_{ij} + h_{ij})dx^i dx^j] \quad (i, j = 1, 2, 3). \quad (\text{A1})$$

$h_{ij}(t, \mathbf{x})$ can be Fourier expanded as

$$h_{ij}(t, \mathbf{x}) = \int \frac{d^3k}{(2\pi)^{3/2}} h_{ij}(t, \mathbf{k}) e^{i\mathbf{k}\cdot\mathbf{x}}, \quad (\text{A2})$$

where $\mathbf{x}(\mathbf{k})$ is the three position (momentum) vector.

The GW spectrum as a function of the conformal time τ and the comoving wave number k is defined to be

$$\Omega_{\text{GW}}(k, \tau) \equiv \frac{1}{\rho_{\text{total}}(\tau)} \frac{d\rho_{\text{GW}}(k, \tau)}{d \log k}, \quad (\text{A3})$$

where $\rho_{\text{total}}(\tau) = 3M_p^2 H(\tau)^2$ is the total energy density of the Universe at the conformal time τ , and $\rho_{\text{GW}}(k, \tau)$ is the energy density of GW. The GW energy density is given by

$$\rho_{\text{GW}} = \frac{1}{32\pi G} \langle \dot{h}_{ij} \dot{h}^{ij} \rangle_V = \frac{1}{32\pi G} \frac{\langle h'_{ij} h'^{ij} \rangle_V}{a^2}, \quad (\text{A4})$$

where the dot (prime) is the derivative with respect to the time t (conformal time τ). Here $\langle \dots \rangle_V$ means the average over a volume of the size of several wavelengths.

In the presence of (traceless and transverse) anisotropic stress T_{ij}^{TT} , which lasts for the time interval $[\tau_i, \tau_f]$, the time evolution of the Fourier component of h_{ij} is given by

$$h''_{ij} + 2\frac{a'}{a} h'_{ij} + k^2 h_{ij} = 16\pi G T_{ij}^{TT}, \quad (\text{A5})$$

where $G \equiv (8\pi M_p^2)^{-1}$ is the Newtonian constant. Having $h_{ij}(\tau_i) = h'_{ij}(\tau_i) = 0$ as the initial condition, the solution to Eq. (A5) for $\tau \in [\tau_i, \tau_f]$ can be obtained by the time integral of T_{ij}^{TT} convoluted with a Green function [67,68]. For the time $\tau > \tau_{\text{RH}} > \tau_f = \tau_{\text{decay}}$, h_{ij} follows the time evolution equation without T_{ij}^{TT} in Eq. (A5) and the solution thereof is given by [52]

$$h_{ij}(\mathbf{k}, \tau) = A_{ij}(\mathbf{k}) \frac{k\tau}{a} j_0(k\tau) + B_{ij}(\mathbf{k}) \frac{k\tau}{a} n_0(k\tau), \quad (\text{A6})$$

where the time independent coefficients $A_{ij}(\mathbf{k})$ and $B_{ij}(\mathbf{k})$ contain information for T_{ij}^{TT} through

$$A_{ij}(\mathbf{k}) = -16\pi G \int_{\tau_i}^{\tau_f} d\tau \tau a(\tau) f_A(k\tau) T_{ij}^{TT}(\mathbf{k}, \tau), \quad (\text{A7})$$

$$B_{ij}(\mathbf{k}) = 16\pi G \int_{\tau_i}^{\tau_f} d\tau \tau a(\tau) f_B(k\tau) T_{ij}^{TT}(\mathbf{k}, \tau), \quad (\text{A8})$$

with the following forms of $f_A(k\tau)$ and $f_B(k\tau)$

$$f_A(k\tau) = a_1 n_1(k\tau) - a_2 j_1(k\tau), \quad (\text{A9})$$

$$f_B(k\tau) = -b_1 n_1(k\tau) + b_2 j_1(k\tau), \quad (\text{A10})$$

where j_1 and n_1 are the spherical Bessel and Neumann function of the first order, respectively. The coefficients a_1 , a_2 , b_1 , and b_2 are given by

$$a_1 = x^2 [j_1(x) \partial_x n_0(x) - n_0(x) \partial_x j_1(x)], \quad (\text{A11})$$

$$a_2 = x^2 [n_1(x) \partial_x n_0(x) - n_0(x) \partial_x n_1(x)], \quad (\text{A12})$$

$$b_1 = x^2 [j_1(x) \partial_x j_0(x) - j_0(x) \partial_x j_1(x)], \quad (\text{A13})$$

$$b_2 = x^2 [n_1(x) \partial_x j_0(x) - j_0(x) \partial_x n_1(x)], \quad (\text{A14})$$

where x is to be evaluated at $x = k\tau_{\text{RH}}$. Finally, after substituting h_{ij} in Eq. (A6) into Eqs. (A4) and (A3), one obtains the spectrum of the GW

$$\Omega_{\text{GW}} \simeq \frac{k^5}{48\pi^2 V a^4 H^2} \sum_{ij} (|A_{ij}|^2 + |B_{ij}|^2). \quad (\text{A15})$$

-
- [1] T. Banks and N. Seiberg, Symmetries and strings in field theory and gravity, *Phys. Rev. D* **83**, 084019 (2011).
- [2] K. Kurosawa, N. Maru, and T. Yanagida, Nonanomalous R symmetry in supersymmetric unified theories of quarks and leptons, *Phys. Lett. B* **512**, 203 (2001).
- [3] M. Dine and J. Kehayias, Discrete R symmetries and low energy supersymmetry, *Phys. Rev. D* **82**, 055014 (2010).
- [4] J. L. Evans, M. Ibe, J. Kehayias, and T. T. Yanagida, Non-Anomalous Discrete R-symmetry Decees Three Generations, *Phys. Rev. Lett.* **109**, 181801 (2012).
- [5] K. Harigaya, M. Ibe, K. Schmitz, and T. T. Yanagida, Peccei-Quinn symmetry from a gauged discrete R symmetry, *Phys. Rev. D* **88**, 075022 (2013).
- [6] M. Dine and A. Monteux, Discrete R symmetries and anomalies, *J. High Energy Phys.* **01** (2014) 011.
- [7] N. Sakai and T. Yanagida, Proton decay in a class of supersymmetric grand unified models, *Nucl. Phys.* **B197**, 533 (1982).
- [8] S. Weinberg, Supersymmetry at ordinary energies. 1. Masses and conservation laws, *Phys. Rev. D* **26**, 287 (1982).
- [9] Y. B. Zeldovich, I. Y. Kobzarev, and L. B. Okun, Cosmological consequences of the spontaneous breakdown of discrete symmetry, *Zh. Eksp. Teor. Fiz.* **67**, 3 (1974).
- [10] T. W. B. Kibble, Topology of cosmic domains and strings, *J. Phys. A* **9**, 1387 (1976).
- [11] M. Dine, F. Takahashi, and T. T. Yanagida, Discrete R symmetries and domain walls, *J. High Energy Phys.* **07** (2010) 003.
- [12] K.-I. Izawa and T. Yanagida, Dynamical supersymmetry breaking in vector-like gauge theories, *Prog. Theor. Phys.* **95**, 829 (1996).
- [13] K. A. Intriligator and S. D. Thomas, Dynamical supersymmetry breaking on quantum moduli spaces, *Nucl. Phys.* **B473**, 121 (1996).
- [14] L. E. Ibanez and G. G. Ross, Discrete gauge symmetry anomalies, *Phys. Lett. B* **260**, 291 (1991).
- [15] L. E. Ibanez and G. G. Ross, Discrete gauge symmetries and the origin of baryon and lepton number conservation in supersymmetric versions of the standard model, *Nucl. Phys.* **B368**, 3 (1992).
- [16] L. E. Ibanez, More about discrete gauge anomalies, *Nucl. Phys.* **B398**, 301 (1993).
- [17] N. Seiberg, Exact results on the space of vacua of four-dimensional SUSY gauge theories, *Phys. Rev. D* **49**, 6857 (1994).
- [18] A. A. Starobinsky, A new type of isotropic cosmological models without singularity, *Phys. Lett.* **91B**, 99 (1980).
- [19] A. H. Guth, The inflationary universe: A possible solution to the horizon and flatness problems, *Phys. Rev. D* **23**, 347 (1981).
- [20] A. D. Linde, A new inflationary universe scenario: A possible solution of the horizon, flatness, homogeneity, isotropy and primordial monopole problems, *Phys. Lett.* **108B**, 389 (1982).
- [21] A. Albrecht and P. J. Steinhardt, Cosmology for Grand Unified Theories with Radiatively Induced Symmetry Breaking, *Phys. Rev. Lett.* **48**, 1220 (1982).
- [22] R. Brandenberger, Initial conditions for inflation—A short review, *Int. J. Mod. Phys. D* **26**, 1740002 (2017).
- [23] W. E. East, M. Kleban, A. Lindem, and L. Senatore, Beginning inflation in an inhomogeneous universe, *J. Cosmol. Astropart. Phys.* **09** (2016) 010.
- [24] A. Vilenkin, Topological Inflation, *Phys. Rev. Lett.* **72**, 3137 (1994).
- [25] Planck Collaboration, Planck 2018 results. X. Constraints on inflation, *Astron. Astrophys.* **641**, A10 (2020).
- [26] BICEP, Keck Collaboration, Improved Constraints on Primordial Gravitational Waves using Planck, WMAP, and BICEP/Keck Observations through the 2018 Observing Season, *Phys. Rev. Lett.* **127**, 151301 (2021).
- [27] M. Ibe and T. T. Yanagida, The lightest Higgs boson mass in pure gravity mediation model, *Phys. Lett. B* **709**, 374 (2012).

- [28] H. P. Nilles, Supersymmetry, supergravity and particle physics, *Phys. Rep.* **110**, 1 (1984).
- [29] G. F. Giudice, M. A. Luty, H. Murayama, and R. Rattazzi, Gaugino mass without singlets, *J. High Energy Phys.* **12** (1998) 027.
- [30] L. Randall and R. Sundrum, Out of this world supersymmetry breaking, *Nucl. Phys.* **B557**, 79 (1999).
- [31] M. Dine and D. MacIntire, Supersymmetry, naturalness, and dynamical supersymmetry breaking, *Phys. Rev. D* **46**, 2594 (1992).
- [32] J. Hisano, S. Matsumoto, M. Nagai, O. Saito, and M. Senami, Non-perturbative effect on thermal relic abundance of dark matter, *Phys. Lett. B* **646**, 34 (2007).
- [33] M. Cirelli, A. Strumia, and M. Tamburini, Cosmology and astrophysics of minimal dark matter, *Nucl. Phys.* **B787**, 152 (2007).
- [34] A. R. Liddle and S. M. Leach, How long before the end of inflation were observable perturbations produced?, *Phys. Rev. D* **68**, 103503 (2003).
- [35] J. B. Munoz and M. Kamionkowski, Equation-of-state parameter for reheating, *Phys. Rev. D* **91**, 043521 (2015).
- [36] J. L. Cook, E. Dimastrogiovanni, D. A. Easson, and L. M. Krauss, Reheating predictions in single field inflation, *J. Cosmol. Astropart. Phys.* **04** (2015) 047.
- [37] M. S. Turner, Coherent scalar-field oscillations in an expanding universe, *Phys. Rev. D* **28**, 1243 (1983).
- [38] T. Yanagida, Horizontal gauge symmetry and masses of neutrinos, *Conf. Proc.* **C7902131**, 95 (1979).
- [39] T. Yanagida, Horizontal symmetry and mass of the top quark, *Phys. Rev. D* **20**, 2986 (1979).
- [40] M. Gell-Mann, P. Ramond, and R. Slansky, Complex spinors and unified theories, *Conf. Proc.* **C790927**, 315 (1979).
- [41] P. Minkowski, $\mu \rightarrow e\gamma$ at a rate of one out of 10^9 muon decays?, *Phys. Lett.* **67B**, 421 (1977).
- [42] M. Fukugita and T. Yanagida, Baryogenesis without grand unification, *Phys. Lett. B* **174**, 45 (1986).
- [43] W. Buchmuller, R. D. Peccei, and T. Yanagida, Leptogenesis as the origin of matter, *Annu. Rev. Nucl. Part. Sci.* **55**, 311 (2005).
- [44] T. Gherghetta, C. F. Kolda, and S. P. Martin, Flat directions in the scalar potential of the supersymmetric standard model, *Nucl. Phys.* **B468**, 37 (1996).
- [45] F. Buccella, J. P. Derendinger, S. Ferrara, and C. A. Savoy, Patterns of symmetry breaking in supersymmetric gauge theories, *Phys. Lett.* **115B**, 375 (1982).
- [46] I. Affleck, M. Dine, and N. Seiberg, Dynamical supersymmetry breaking in supersymmetric QCD, *Nucl. Phys.* **B241**, 493 (1984).
- [47] I. Affleck, M. Dine, and N. Seiberg, Dynamical supersymmetry breaking in four-dimensions and its phenomenological implications, *Nucl. Phys.* **B256**, 557 (1985).
- [48] I. Affleck and M. Dine, A new mechanism for baryogenesis, *Nucl. Phys.* **B249**, 361 (1985).
- [49] G. Choi, M. Suzuki, and T. T. Yanagida, Degenerate fermion dark matter from a broken $U(1)_{B-L}$ gauge symmetry, *Phys. Rev. D* **102**, 035022 (2020).
- [50] G. Choi, T. T. Yanagida, and N. Yokozaki, Dark photon dark matter in the minimal $B - L$ model, *J. High Energy Phys.* **01** (2021) 057.
- [51] A. Kamada and M. Yamada, Gravitational waves as a probe of the SUSY scale, *Phys. Rev. D* **91**, 063529 (2015).
- [52] A. Kamada and M. Yamada, Gravitational wave signals from short-lived topological defects in the MSSM, *J. Cosmol. Astropart. Phys.* **10** (2015) 021.
- [53] K. Enqvist and J. McDonald, Q balls and baryogenesis in the MSSM, *Phys. Lett. B* **425**, 309 (1998).
- [54] E. W. Kolb and M. S. Turner, *Front. Phys.* **69**, 1 (1990).
- [55] D. J. H. Chung, E. W. Kolb, and A. Riotto, Production of massive particles during reheating, *Phys. Rev. D* **60**, 063504 (1999).
- [56] N. Seto and J. Yokoyama, Probing the equation of state of the early universe with a space laser interferometer, *J. Phys. Soc. Jpn.* **72**, 3082 (2003).
- [57] K. Nakayama, S. Saito, Y. Suwa, and J. Yokoyama, Space laser interferometers can determine the thermal history of the early Universe, *Phys. Rev. D* **77**, 124001 (2008).
- [58] M. Punturo *et al.*, The Einstein telescope: A third-generation gravitational wave observatory, *Classical Quant. Grav.* **27**, 194002 (2010).
- [59] D. Reitze *et al.*, Cosmic explorer: The U.S. contribution to gravitational-wave astronomy beyond LIGO, *Bull. Am. Astron. Soc.* **51**, 035 (2019).
- [60] C. Périgois, C. Belczynski, T. Bulik, and T. Regimbau, StarTrack predictions of the stochastic gravitational-wave background from compact binary mergers, *Phys. Rev. D* **103**, 043002 (2021).
- [61] LIGO Scientific, VIRGO Collaborations, Search for the isotropic stochastic background using data from Advanced LIGO's second observing run, *Phys. Rev. D* **100**, 061101 (2019).
- [62] LIGO Scientific Collaborations, Advanced LIGO, *Classical Quant. Grav.* **32**, 074001 (2015).
- [63] LIGO Scientific Collaborations, Gravitational waves from known pulsars: Results from the initial detector era, *Astrophys. J.* **785**, 119 (2014).
- [64] KAGRA Collaborations, Interferometer design of the KAGRA gravitational wave detector, *Phys. Rev. D* **88**, 043007 (2013).
- [65] C. S. Unnikrishnan, IndIGO and LIGO-India: Scope and plans for gravitational wave research and precision metrology in India, *Int. J. Mod. Phys. D* **22**, 1341010 (2013).
- [66] L. M. Krauss and F. Wilczek, Discrete Gauge Symmetry in Continuum Theories, *Phys. Rev. Lett.* **62**, 1221 (1989).
- [67] J. F. Dufaux, A. Bergman, G. N. Felder, L. Kofman, and J.-P. Uzan, Theory and numerics of gravitational waves from preheating after inflation, *Phys. Rev. D* **76**, 123517 (2007).
- [68] M. Kawasaki and K. Saikawa, Study of gravitational radiation from cosmic domain walls, *J. Cosmol. Astropart. Phys.* **09** (2011) 008.